Additive Manufacturing 28 (2019) 87–97

Contents lists available at ScienceDirect

Additive Manufacturing

journal homepage: www.elsevier.com/locate/addma

A review of the fatigue behavior of 3D printed polymers

Lauren Safai*, Juan Sebastian Cuellar, Gerwin Smit, Amir A. Zadpoor

Department of Biomechanical Engineering, Faculty of Mechanical, Maritime and Materials Engineering, Delft University of Technology, Mekelweg 2, Delft, 2628CD, the Netherlands

ARTICLE INFO

Keywords:
3D printing
Polymers
Mechanical behavior
Cyclic loading
Fatigue fracture

ABSTRACT

As additive manufacturing of polymeric materials is becoming more prevalent throughout industry and research communities, it is important to ensure that 3D printed parts are able to withstand mechanical and environmental stresses that occur when in use, including the sub-critical cyclic loads that could result in fatigue crack propagation and material failure. There has so far been only limited research on the fatigue behavior of 3D printed polymers to determine which printing or material parameters result in the most favorable fatigue behavior. To better understand the effects of the printing technique, printing materials, and printing parameters on the fatigue behavior of 3D printed materials, we present here an overview of the data currently available in the literature including fatigue testing protocols and a quantitative analysis of the available fatigue data per type of the AM technology. The results of our literature review clearly show that, due to the synergism between printing parameters and the properties of the printed material, it is challenging to determine the best combination of variables for fatigue resistance. There is therefore a need for more experimental and computational fatigue studies to understand how the above-mentioned material and printing parameters affect the fatigue behavior.

1. Introduction

The use of additive manufacturing (AM), or 3D printing, has been increasing due to the growing interest from both industry and research communities [1]. As additive manufacturing technology improves, high quality prints can be produced quickly and inexpensively. With a wider range of polymer materials available, the development and fabrication of products are continuously changing with technological advancement and consumer use [1]. Innovators and inventors are now able to build prototypes or complex geometries efficiently at minimal costs with the reduction of production time from weeks to hours [2]. As a result of these improvements in AM, various industries such as biomedical [3–10], aerospace [11], apparel [12,13], dentistry [14], automotive [15], electronics [2,16], and oceanography [17] are researching this technique to produce parts.

As additive manufacturing becomes more widely used, parts must withstand both mechanical and environmental stresses that occur during use. Understanding the required strengths for specific loading conditions is vital for any load-bearing applications [18,19]. Since a material may fail due to fatigue conditions, it is also important to understand a material's resistance to cyclic loading and unloading [20]. Repetitive sub-critical loading of material may result in fatigue damage, i.e. a progressive accumulation and permanent structural change, which could lead to cracking or rupturing of the part after a certain number of cycles. Polymers are susceptible to fatigue at applied stresses below yield, which can cause microcracking and eventual failure [21]. Understanding the fatigue behavior of AM parts is therefore essential for predicting and preventing fatigue failure.

This paper will review current literature investigating the fatigue life of 3D printed polymers (Appendix A). The aim is to see if there are trends between experiments that provide insight into which printing parameters and material properties lead to the best fatigue life for 3D printed polymers.

2. Fatigue

As previously mentioned, fatigue is the development of structural damage as a result of repetitive loads (i.e. cyclic loading) that are less than ultimate tensile strength and possibly yield strength. Fatigue failure in polymers occurs in two ways [22,23]: (1) thermal failure due to softening and melting from hysteretic heating, or (2) mechanical failure from crack initiation and propagation. As a result of high damping, viscoelasticity, and low thermal conductivity, high frequencies or strain rates cause hysteretic heating in thermal fatigue [24,25]. The hysteretic energy is mainly dissipated as heat, which causes the specimen temperature to increase and the stiffness to

* Corresponding author.
E-mail address: lsafai03@gmail.com (L. Safai).

https://doi.org/10.1016/j.addma.2019.03.023
Received 26 October 2018; Received in revised form 19 March 2019; Accepted 23 March 2019
Available online 06 April 2019

decrease. Stiffness loss causes an increase in specimen deflection and deformation. From a macroscopic viewpoint, the process of fatigue failure in polymers resembles that of metals [26,27]: it starts with initial microcracks on the surface or stress concentrator that grow into macroscopic cracks and cause the final failure. Depending on the type of polymer, the crack may originate in different ways. In semi-crystalline polymers, for example, the crack is likely to initiate in spherulites. Once the crack growth enters the micro-structurally independent stage, the crack continues until the final rupture of the material [28,29]. According to reference [30], thermal failure does not necessarily have a crack at failure, while mechanical failure is a result of physical separation.

3. Fatigue testing

3.1. Objectives of fatigue testing

There are several objectives when fatigue testing: material type testing, structural type testing, and actual service type testing [31]. Material testing investigates the material response to repeated stresses, various environments, geometrical factors, or surface finishes. In structural testing, different materials or structural designs are tested to analyze stress concentrations, fatigue life, or fabrication processes. Finally, actual service type testing is used for reliability or quality verification.

3.2. Types of fatigue testing

Fatigue testing machines are classified based on the applied stress method. For axial loading, a uniform stress or strain is directly applied to the cross-section of the specimen in tension or compression. The specimen is held at both ends and loaded cyclically between minimum and maximum values. During repeated or reciprocating bending, one end of the specimen is fixed while a stress or strain is applied to the other end such that the specimen bends in the same plane. In rotating bending, the specimen is revolved at a constant frequency while a load is applied at two clamping points on the either side of the specimen. In every rotational cycle, the stresses change from compressive to tensile and from tensile to compressive, making sure that the specimen experiences the full cycle of flexural stresses. For fracture mechanical testing, a notch is made in the specimen to examine fracture initiation and propagation during cyclic loading. In torsion fatigue, each end of the specimen is either clamped or twisted to specified values through a stress or strain. Other types of fatigue tests include combined bending and torsion fatigue and biaxial and triaxial fatigue, which are used in more complicated fatigue analyses [31,32].

3.3. Stress amplitude in fatigue testing

The simplest stress sequence uses a constant stress amplitude where all load cycles, or cycles, are identical (Fig. 1). For each cycle, σ is the alternating stress, σ_m is the mean stress, σmax is the maximum stress, and σmin is the minimum stress. Load cycles can be expressed as $\sigma_m \pm \sigma$, with compressive loads taken as negative. It follows that:

$$\sigma_{max} = \sigma_m + \sigma \tag{1}$$

$$\sigma_{min} = \sigma_m - \sigma \tag{2}$$

$$\sigma_m = \frac{\sigma_{min} + \sigma_{max}}{2} \tag{3}$$

For constant amplitude loading, the stress range, S, and stress ratio, R, are expressed as:

$$S = 2\sigma = \sigma_{max} - \sigma_{min} \tag{4}$$

$$R = \frac{\sigma_{min}}{\sigma_{max}} \tag{5}$$

Depending on stress level, constant amplitude loading can be classified into several different testing categories [31]. Routine tests are chosen so the specimen fails at a moderate number of cycles (i.e. 10^4-10^7). In short-life tests, applied stress is chosen to surpass yield stress so statistically some specimens fail at the application of the load, while in long-life tests, load is set to be just above or below the fatigue limit so some specimens do not fail after an assigned number of cycles. The aim of the long-life test is to examine the distribution of fatigue strength at a pre-assigned cycle number, which is beneficial for determining the fatigue limit.

In contrast to constant amplitude loading, variable amplitude loading (Fig. 2) has complicated loading sequences that are more realistic to what structures and components experience [28,31]. Variable loading is used for cumulative damage analysis or the simulation of service life. Cumulative damage testing is performed at several stress levels with a simplified loading sequence, while service simulations have a more complicated loading pattern [31].

3.4. Stressing sources

In fatigue testing, force-controlled or displacement-controlled methods can be implemented, which is where a specific force or displacement is increased and decreased at a specified and controlled rate, respectively. Loads are produced by one of the following techniques: mechanical deflections, dead weights or constant springs, centrifugal forces, electromagnetic forces, hydraulic forces, or pneumatic forces. Load choice depends on factors such as frequency, control systems, required forces, costs, and simplifications of working loads [31].

3.5. Presentation of fatigue data

During fatigue testing, cyclic loads are applied with varied or constant stresses, which can be either positive or negative. A series of fatigue tests are conducted at several stress levels to create a stress-cycle plot or S-N curve, which is the conventional method of presenting fatigue behavior of polymers. Since current theories do not explain the mechanical behavior of polymers, empirical methods have been applied to analyze polymer fatigue [33]. S-N curves plot the stress endured against the number of cycles until failure. By lowering the stress value during testing, a fatigue limit can be established with the S-N curve, which is a value that does not result in failure and is sometimes referred to as fatigue limit, endurance limit, or fatigue strength [28]. The fatigue limit is affected by material surface conditions, such as roughness, damage, treatment, and residual stresses [28].

4. Fatigue testing machines and specimens

4.1. Components

Each fatigue-testing machine consists of the same basic structural components: (1) a load train that consists of a load-producing mechanism to generate the desired load or displacement and a load-transmitting mechanism to produce the desired stress distribution; (2) controllers to set the upper and lower load limits and maintain the load throughout the test; (3) a counting and shut-off apparatus to stop the machine after failure or the pre-assigned number of cycles; and (4) a framework to support all of the necessary parts and reduce vibrations in the system [31,32].

4.2. Specimens

Fatigue test specimens typically have three sections, including two grip ends and the test section [32]. The grips of the specimen are designed to transfer load from the test machine to the test section, and, depending on the test, may not be identical. Transitions between the grips and test section are designed with large radii so no stress

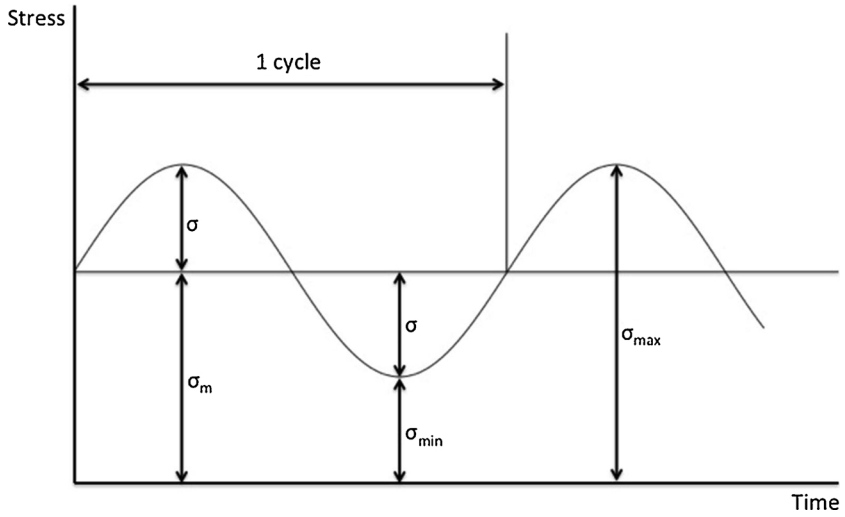

Fig. 1. Nomenclature that describes testing parameters in constant amplitude loading.

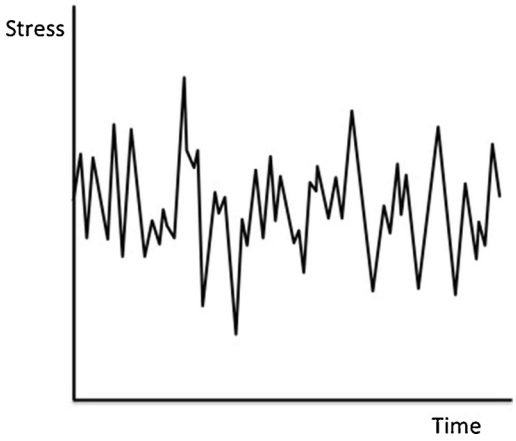

Fig. 2. An example of a general variable amplitude loading.

concentrations build-up. The desired type of test and the objectives affect the design of the fatigue test specimen. Several fatigue test specimens are shown in Fig. 3.

5. Fatigue testing of 3d printed polymers

5.1. Factors affecting fatigue characterization

Fatigue testing in 3D printed specimens is challenging due to the anisotropic properties and residual stresses that result from layer deposition [19]. Different variables associated with each type of printing technique affect the mechanical characterization of the specimens. The variables for extrusion-based printing include: raster orientation, build orientation, layer height and bead width, and air gap between filaments [19,34–37]. The mechanical properties of powder bed fusion-based specimens are affected by the laser power, scan length, layer height, build orientation, recycled powder content, powder bed temperature, and crystallization temperature [19,38]. Parts printed with material jetting techniques are affected by the presence of additives, unknown manufacturer resin formulations, printed on an over-cured surface, and the physics and chemistry of polymer fusion [19]. Due to the synergism between these variables, fatigue is challenging to predict. All of these variables influence the microstructure of the part that, in turn, may significantly affect the mechanical behavior and failure mechanism. There was no literature regarding the fatigue testing of polymers fabricated using other categories of 3D printing techniques.

5.2. Standardization of fatigue testing

The American Society for Testing and Materials (ASTM) and the International Standards Organization (ISO) are two institutes that address the standardization of mechanical testing of AM specimens [19]. Currently, there is limited standardization in terms of the fatigue testing of 3D printed polymers.

With no ISO equivalent, the ASTM D7774 standard addresses uniaxial fatigue in tension or compression [39]. While it is recommended

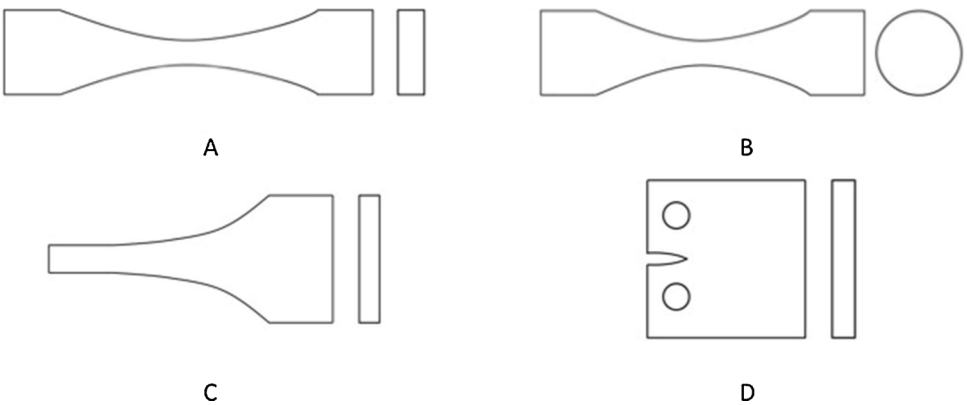

Fig. 3. Four examples of fatigue testing specimens that include A) an axial loading specimen, B) a rotating bending specimen, C) a reverse bending specimen, and D) a fracture mechanical test specimen.

to test below a frequency of 5 Hz to reduce heat generation, specimens can be cycled between 1–25 Hz. The fatigue limit is defined when the specimen fails or reaches 10^7 cycles. Stress or strain is applied so the material does not experience plastic behavior. In addition to the previous standard, ASTM D3479 investigates tension fatigue for polymer matrix composites for specific loading and environmental conditions [40].

Two standards, ASTM D7791 and ISO 13003, address flexural fatigue in plastics [41,42]. Both standards have sinusoidal loading, but are technically different. ASTM D7791 tests specimens using three- or four-point bending, while ISO 13003 is applicable to all testing methods. For ASTM D7791, cyclic loading alternates between positive and negative values so that R is -1 and the stress or strain remains within the elastic limit. The fatigue limit is characterized in the same fashion as the previous standard. In ISO 13003, fiber-reinforced plastic composites undergo cyclic loading at a constant amplitude and frequency at four different stress or strain levels. For displacement control, the termination of the test is characterized as reaching the cycle limit or the specimen stiffness is reduced by 20%.

There are two standards, ASTM D6115 and ISO 15850, that address crack propagation (fatigue delamination) in the interlaminar region of a fiber composite [43,44]. Since both standards are defined specifically for composites, it is unclear if 3D printed materials would fulfill the supporting assumptions. Finally, in order to perform statistical analyses of fatigue data, the standard ASTM E739 can be used [45].

6. Analysis of fatigue experiments

This section reviews the literature associated with the fatigue testing of 3D printed polymers, namely those printed using extrusion-based printing, selective laser sintering, and material jetting (e.g., polyjet printing). The topics of interest include the effects of printing parameters, material properties, production methods, and geometric considerations on the fatigue life. Tables 1–3, following each section, summarize the experiments of each study and the conclusions drawn about fatigue life.

6.1. Extrusion-based printing

6.1.1. Axial loading fatigue

Various printing parameters, such as raster orientation, printing orientation, layer thickness, and feed rate, have been found to influence fatigue life of 3D printed parts. In several studies conducted by Ziemian et al., the effects of raster orientation were examined when printing with acrylonitrile butadiene styrene (ABS) [46–48]. In the first study [46], rectangular prism specimens ($190 \times 12.7 \times 2.6$ mm^3) were printed with four raster orientations of 0° (Fig. 4A), 45° (Fig. 4C), 90° (Fig. 4B), and 45°/45° (Fig. 4D). The results indicated that the 45°/45° raster orientation has the best fatigue life. In the subsequent studies [47,48], ASTM D638 dog bone specimens were printed with raster orientations of 0° (Fig. 4A), 45° (Fig. 4C), 90° (Fig. 4B), 45°/45° (Fig. 4D), 30°/60°, 15°/75°, and 0°/90° (for conventions used in defining raster orientations, see Fig. 4) [49]. In accordance with the first study, the 45°/45° raster orientation exhibited the best performance (Fig. 6).

Both [50] and [51] investigated the effects of raster orientation, but in polylactic acid (PLA) specimens according to references [41] and [49], respectively. Three raster orientations of 0° (Fig. 4A), 45° (Fig. 4C), and 90° (for conventions used in defining raster orientations, see Fig. 4) (Fig. 4B) were cyclically loaded at 2 Hz in [50] and 1 Hz in reference [51]. Both studies had similar results, where the 45° orientation had the best fatigue life. In a different study [52], the effects of printing orientation on fatigue life in ABS and ABS*plus* specimens [53] were investigated. Nine specimens were printed in varying directions, where each print orientation dictated the raster orientation used by the printer (Fig. 5). It was found that printing the specimen in the Flat-x (Fig. 5) direction had the best fatigue life. In Fig. 6, the S-N curves for the best results from [47,50–52] are presented. From the curves, it can be concluded that ABS*plus* had better fatigue resistance than ABS since, at each stress level, the ABS*plus* material had a larger number of cycles. Comparing ABS and PLA, it was inconclusive which material had the better fatigue life, since the PLA and ABS curves between studies provided conflicting results. Finally, in a cumulative study, reference [54] explored which printing parameter (layer thickness, extruder width, print orientation, feed rate) has the most influence on the fatigue life. Rectangular prisms ($150 \times 20 \times 3$ mm) of ABS were tested with 0.2 or 0.3 mm layer thickness, 0.35 or 0.45 mm extruder width, Flat-x or Flat-y (Fig. 5) print orientation, and 2000 or 4000 mm/min feed rate. It was found that printing in the Flat-x direction and using a smaller layer height resulted in the best fatigue life. For feed rate and extruder width, while it appeared that smaller values resulted in better fatigue life, neither parameter had a significant impact on fatigue life. Printing parameters were found to have a substantial impact on the fatigue life in polymers.

Material properties and production methods, such as fabrication with injection molding or 3D printing and surface treatments, were investigated to see how fatigue life was affected. Both [55] and [56] studied and compared the fatigue lives of injection molded and 3D printed specimens [49] of ABS and polycarbonate urethane (75 A, 85 A, and 95 A), respectively. In conflicting results [55], found that the 3D printed specimens had worse fatigue life, while [56] found that 3D printed parts had a better fatigue life (Fig. 7 and 8). From Figs. 7 and 8, it can be seen that the ABS injected molded specimens had the best

Table 1
A summary of fatigue testing parameters and results from the studies that used extrusion-based printing.

Testing Method	Material	Specimen Geometry	Results	Study
Tension-tension fatigue	ABS	Rectilinear Box	The 45°/45° fiber orientation had the best fatigue life	Ziemian et al. (2012)
Tension-tension fatigue	ABS	Dog Bone	The 45°/45° fiber orientation had the best fatigue life	Ziemian et al. (2015)
Tension-tension fatigue	ABS	Dog Bone	The 45°/45° fiber orientation had the best fatigue life	Ziemian et al. (2016)
Tension-tension fatigue	PLA	Dog Bone	Flat printing orientation at 45° had the best fatigue life	Afrose et al. (2015)
Tension-compression fatigue	PLA	Dog Bone	Flat printing orientation at 45° had the best fatigue endurance limit	Letcher and Waytashek (2014)
Tension-relaxation fatigue	ABS	Dog Bone	Flat printing orientation in X had the best fatigue life	Lee and Huang (2013)
Tension-tension fatigue	ABS	Rectilinear Box	Print orientation, layer thickness, and feed rate influenced fatigue life the most	Corbett et al. (2014)
Tension-tension fatigue	ABS	Dog Bone	3D-printed parts had worse fatigue life than injection molding	Padzi et al. (2017)
Tension-relaxation fatigue	Polycarbonate Urethane	Dog Bone	3D-printed parts had better fatigue life than injection molding	Miller et al. (2017a)
Tension-tension fatigue	Ultem 9085	Dog Bone	Surface treatment did not affect fatigue life	Fischer and Volker (2016)
Tension-relaxation fatigue	Polyurethane	Rectilinear Box	Circular pores had the best fatigue life	Miller et al. (2017b)
Compression Fatigue	PLA	Rectilinear Box	Circular pores had the best fatigue life	Gong et al. (2017)
Rotating Bending Fatigue	PLA	Hourglass	Fill density and layer height influenced fatigue life the most	Gomez-Gras et al. (2018)
Rotating Bending Fatigue	ABS	Hourglass	Cycling at higher stresses led to worse fatigue life	Zhang et al. (2017)
Fracture Mechanical Fatigue	PLA	Compact Tension	The 0°/90° fiber orientation had the best fatigue life	Arbeiter et al. (2018)

Table 2
A summary of fatigue testing parameters and results from the studies that used selective laser sintering.

Testing Method	Material	Specimen Geometry	Results	Study
Tension-compression fatigue	PA12	Hourglass	Orientation did not affect fatigue life, but notched specimens performed better than un-notched	Hooreweder and Kruth (2014)
Tension-tension fatigue Tension-compression fatigue	PA12	Dog Bone	Density and surface roughness did not affect fatigue life	Amel et al. (2014)
Tension-compression fatigue	PA12	Hourglass	Lower density samples led to more crack initiation	Hooreweder et al. (2010)
Tension-compression fatigue	PA12	Hourglass	3D-printed specimens had similar fatigue life to injection molded samples	Hooreweder et al. (2013)
Tension-tension fatigue Tension-compression fatigue	PA12	Dog Bone	Fatigue life increased with section thickness, and larger section thicknesses depended on density	Amel et al. (2016)
Rotating Bending Fatigue	PA12	Hourglass	Specimens had an endurance limit of 15 MPa	Munguia and Dalgarno (2014)
Rotating Bending Fatigue	PA12	Hourglass	Specimens showed isotropic material behavior	Munguia and Dalgarno (2015)
Bending Fatigue	PCL	Rectilinear Box	Smaller particles with a higher degree of sintering had better fatigue life	Salmoria et al. (2014)
Bending Fatigue	PA6/PA12	Rectilinear Box	There was poor affinity between PA6 and PA12	Salmoria et al. (2012)
Bending Fatigue	PA12/PBT	Rectilinear Box	The 90%/10% blend of PA12/PBT had the best fatigue life	Salmoria et al. (2018)
Fracture Mechanical Fatigue	PA12	Compact Tension	3D-printed specimens had a longer fatigue life than injection molded	Blattmeier et al. (2012)
Fracture Mechanical Fatigue	Neat PA12 and PA12-f	Rectilinear Box	PA12-f had better fatigue life at lower temperatures	Salazar et al. (2014a)
Fracture Mechanical Fatigue	PA12 and PA11	Rectilinear Box	Independent of environment and temperature, PA11 had better fatigue life than PA12	Salazar et al. (2014b)

fatigue life, but the injection molded polycarbonate specimens had a slightly worse fatigue life when compared with their 3D printed counterparts. In the case of polycarbonate urethane, the authors argued that the high temperature and cooling process of the 3D printing process may have affected the internal structures of the samples, thereby increasing its capacity to experience strain crystallization. This would lead to less strain hardening effects and could explain the small improvements in the fatigue behavior of 3D printed specimens. Overall, it was unclear whether or not injection molding had better fatigue resistance than 3D printing, since each study drew a different conclusion. Overall, it was unclear whether or not injection molding had better fatigue resistance than 3D printing, since each study drew a different conclusion. Aside from comparing injection molding and 3D printing, reference [57] examined the differences in chemically post-treated and non-treated specimens from the commercially available polymer Ultem 9085. Ultem 9085 is manufactured by Stratasys, and is a high-performance thermoplastic composed of a polyetherimide and polycarbonate copolymer blend (Stratasys Ltd., Minnesota, USA). The results indicated that surface treatment did not have an effect on fatigue life.

Finally, the effects of topological design on the fatigue behavior of 3D printed porous scaffolds have been investigated in a few studies. In one of these studies [58], the effects of pore geometry and notch shape on the fatigue life in polycarbonate urethane (95 A) and polyurethane 68 A (EPU40) dog bone specimens was investigated, while another study [59] examined the effects of scaffold geometry in PLA. The test results from [58] indicated that pore geometry influenced fatigue life, with circular pore geometry and a circular notch shape having the best performance. In accordance with [58,59,61], also found that pore geometry affected fatigue life with a greater influence at high cycles. As well, for a crosshatch pattern, line spacing had a negligible effect on fatigue life.

6.1.2. Rotating bending fatigue

The influence of four different printing parameters, i.e. layer height (0.1, 0.2, 0.3 mm), fill density (25, 50, 75%), nozzle diameter (0.3, 0.4, 0.5 mm), and printing velocity (25, 30, 35 mm/min), were examined in [60] for two different infill patterns, i.e. rectilinear and honeycomb, in cylindrical, PLA test specimens. Fill density was found to have the most impact on fatigue life, while the effects of the layer height and nozzle diameter were dependent on the infill pattern, and velocity did not have a significant impact on fatigue. According to the authors, certain values of the layer height and nozzle diameter lead to an insufficient cohesion between layers, resulting in a reduced fatigue life. The influence of density was not linear between the three values, with the jump from 50 to 75% density having a larger impact. The best combination of parameters was 75% density, 0.5 mm nozzle diameter, 0.3 mm layer height, and a honeycomb infill.

Reference [61] examined the mechanical properties of how cylindrical ABS specimens failed during fatigue testing. Each test specimen broke at the smallest cross section with both static and fatigue fractures. As stress was increased, the amount of static fatigue also increased.

ABS had better a fatigue life as compared with PLA in rotating bending fatigue (Fig. 9), since at higher stress levels, the ABS specimens were able to last for a larger number of cycles.

6.1.3. Fracture mechanical fatigue

In reference [62], the effects of raster orientation on fatigue life in PLA compact tension specimens were examined. The specimens were printed in three different orientations with 0° (Fig. 4A), 90° (Fig. 4B), and 0°/90° (for conventions used in defining raster orientations, see Fig. 4). The study concluded that raster orientation did not affect fatigue life, and that the fatigue behavior was dominated by crack propagation at high loads, and crack initiation at low loads.

Table 3
A summary of fatigue testing parameters and results from the studies that used material jetting.

Testing Method	Material	Specimen Geometry	Results	Study
Tension-tension fatigue	Veroclear 720	Dog Bone	Build orientation affected fatigue life	Suresh et al. (2017)
Tension-relaxation fatigue	TangoBlackPlus	Dog Bone	Interface specimens had a higher fatigue life than no interface	Moore and Williams (2012)
Tension-relaxation fatigue	TangoBlackPlus	Dog Bone	“Glossy” finish specimens had a longer fatigue life than matte finish	Moore and Williams (2015)

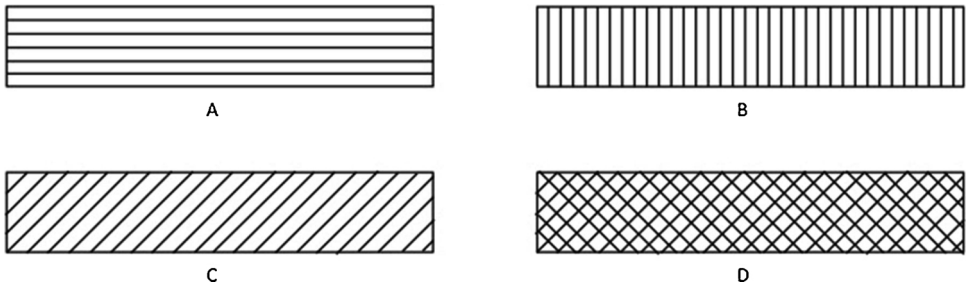

Fig. 4. Four different raster orientations of A) 0°, B) 90°, C) 45°, and D) 45°/45°.

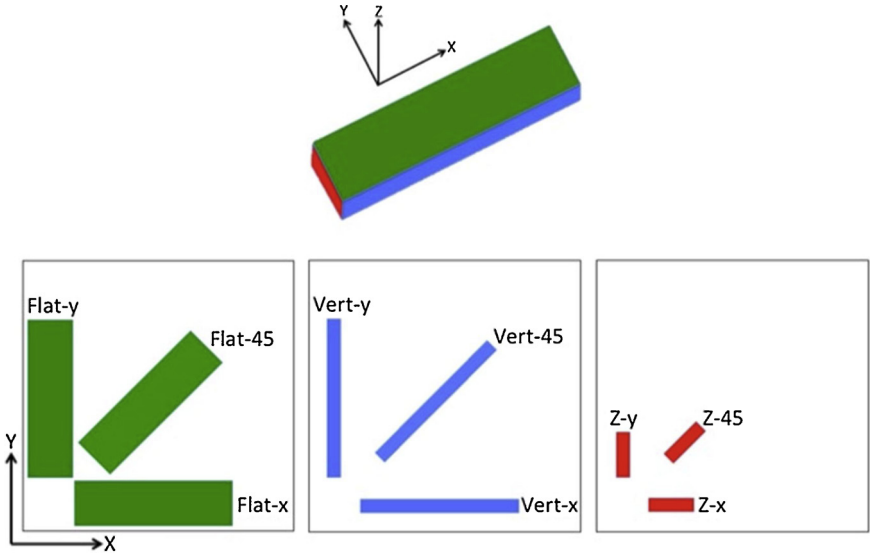

Fig. 5. An arbitrary geometry that shows the notation of the nine different printing orientations on an XYZ stage.

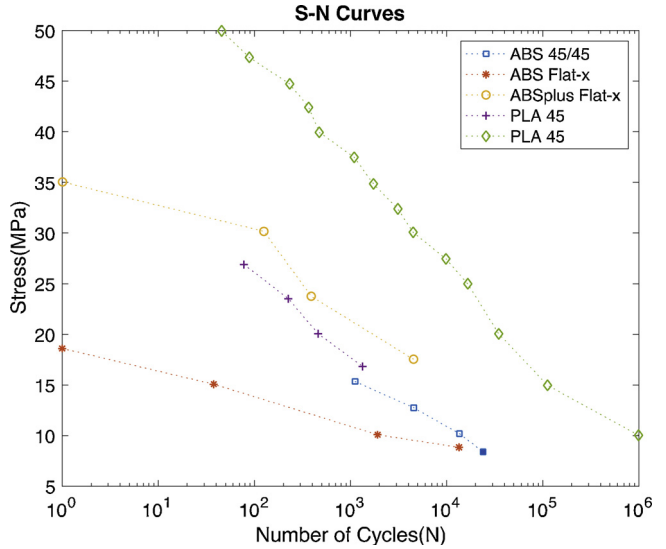

Fig. 6. The S-N curves of the best raster and printing orientation experiments that used dog bone specimens during uniaxial loading. The blue square is the best raster orientation at 45°/45° for ABS specimens [49]. The red star and yellow circle lines are the best printing orientation, flat-x, for ABS and ABS*plus*, respectively [54]. The purple cross and green diamond lines are the best raster orientation at 45° for PLA specimens, from [53] and [52], respectively. Solid color points represent run-out data (For interpretation of the references to colour in this figure legend, the reader is referred to the web version of this article).

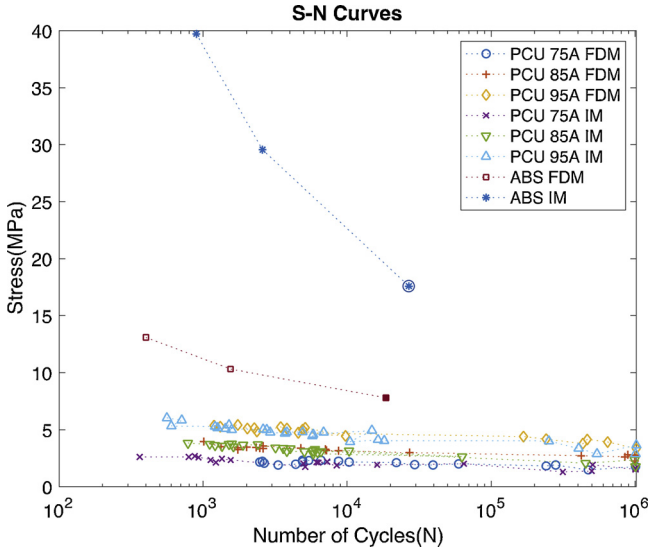

Fig. 7. The S-N curves of the results from [57] and [58] using dog bone specimens made of ABS or polycarbonate urethane, respectively. The blue star and red square curves are the ABS specimens fabricated with 3D printing and injection molding (IM), respectively. The remaining curves are the results of the polycarbonate urethane specimens made with 3D printing and injection molding, which are shown enlarged in the following figure. Solid color points and circled points represent run-out data (For interpretation of the references to colour in this figure legend, the reader is referred to the web version of this article).

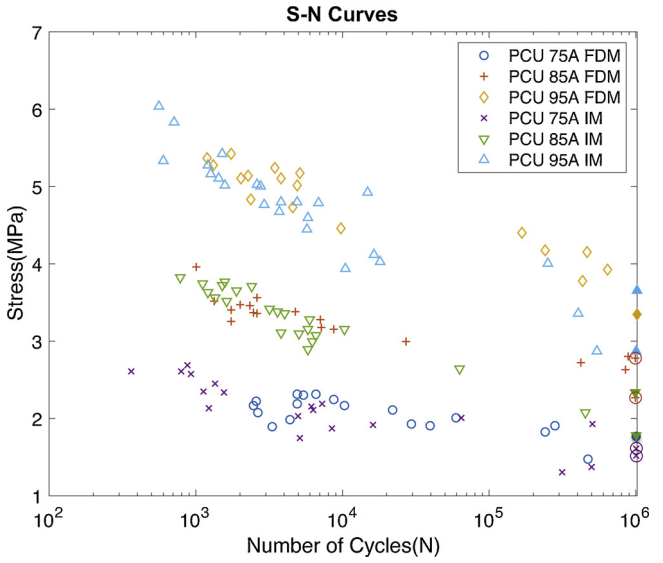

Fig. 8. The S-N curves of the polycarbonate urethane 3D printed and injection molded (IM) specimens for [58]. The specimens were printed in three different types of polycarbonate urethane, 75 A, 85 A, and 95 A. The blue circle, red cross, and yellow diamond are the curves of the 3D printed specimens made with 75 A, 85 A, and 95 A, respectively. The purple cross, downward green triangle, and upward blue triangle are the injection molded specimens made of 75 A, 85 A, and 95 A, respectively. Solid color points and circled points represent run-out data (For interpretation of the references to colour in this figure legend, the reader is referred to the web version of this article).

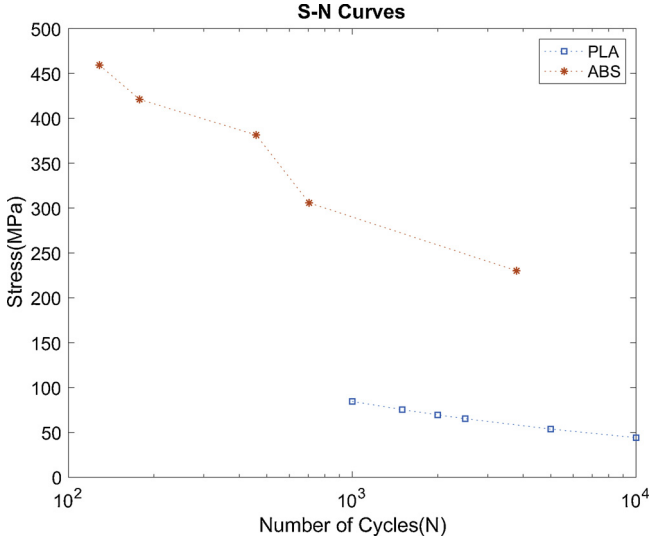

Fig. 9. The S-N curves for the best combination of printing parameters from [62] for PLA hourglass and ABS hourglass specimens from [63]. The red star curve represents the ABS specimen, while the blue square represents the PLA specimen (For interpretation of the references to colour in this figure legend, the reader is referred to the web version of this article).

6.2. Selective laser sintering

6.2.1. Axial loading fatigue

Similar to extrusion-based printing, printing parameters, such as printing orientation, affect parts built using selective laser sintering. In one study [63], the effects of printing orientation on notched and un-notched Nylon-12 (PA12) hourglass specimens [64] were investigated. The results indicated that orientation does not affect the fatigue life, but that notched specimens had a longer fatigue life. This is a result of the reduced thermal load that the notched specimens experience, since a smaller volume is subjected to cyclic loading.

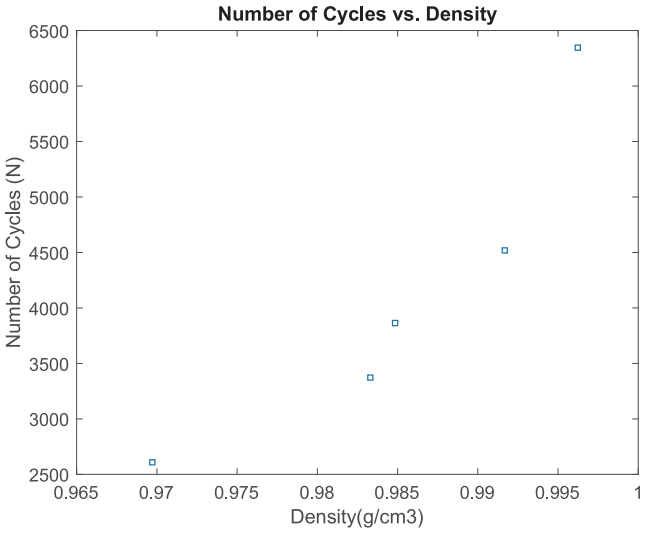

Fig. 10. The results of [68], indicating that as part density increases so does the number of cycles that the specimen is able to withstand.

In addition to printing parameters, material properties, such as density, surface roughness, and printing with injection molding or 3D printing, also influence fatigue life. Studies conducted by [65] and [66] investigated the effects of density on the fatigue life. According to reference [65], there is no relationship between the fatigue life and density or surface roughness in the dog bone Nylon-12 (PA12), since different samples provided contrasting behaviors. In order to verify whether fabrication defects caused this, more testing was needed. However [66], concluded that lower density PA12 hourglass specimens had a lower fatigue life (Fig. 10). As seen from the curve, there was a positive relationship between the density and fatigue life. Aside from density, reference [67] studied the differences in the fatigue life between notched and un-notched injection molded and 3D printed PA12 parts [64], where the 3D printed parts were built in the Vert-x and Z-x directions (Fig. 5). The results found that notched injection molded and 3D printed parts had similar fatigue lives (Fig. 11). Moreover, there were no substantial differences in the fatigue life of the specimens printed in the Vert-x and Z-x directions when using SLS.

In [68], the effects of geometry on the fatigue life was investigated by varying the section thickness (2, 4, and 6 mm) in dog bone PA12 specimens under tension-tension and tension-compression uniaxial loading. In both cases, the fatigue life increased with the section thickness, but these results were not statistically significant for tension-tension loading. This may be due to temperature increasing more in smaller section thicknesses than in larger thicknesses.

6.2.2. Rotating bending fatigue

The effects of printing orientation was investigated in references [69] and [70] for PA12 hourglass specimens [71]. In reference [69], the specimens were printed in the direction of the X and Z-axes (Fig. 5) and tested at two frequencies of 30 and 50 Hz. The results indicated that printing in the Z direction, though not significant, and testing at 50 Hz both reduced fatigue life (Fig. 12). In reference [70], specimens for rotating bending [71] and reverse bending [72] were printed parallel to the Y and Z-axes (Fig. 5). The results of both types of tests and orientations showed no significant differences, indicating isotropic behavior from the specimens (Fig. 12). The curves seen in Fig. 12 include both printing orientations that were tested.

6.2.3. Bending fatigue

In [73], two printing parameters, namely laser energy density and particle size, were varied to see their influence on the fatigue life of

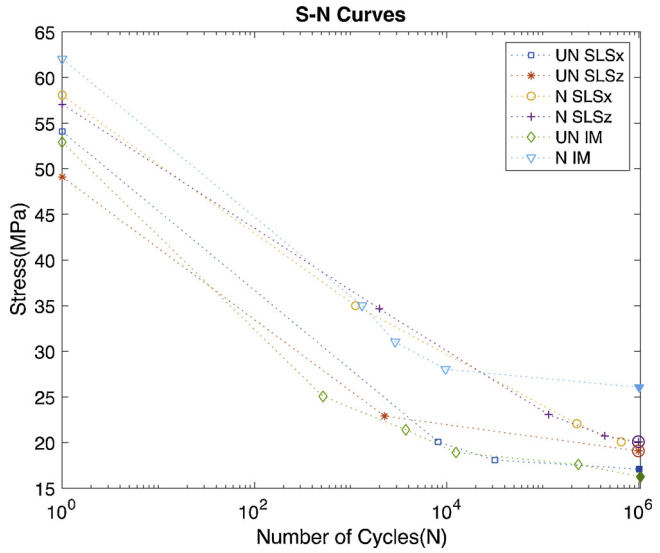

Fig. 11. The S-N curves of the results from [69] using notched and un-notched hourglass specimens of PA12 fabricated using SLS or injection molding (IM). The blue square and red star curves are the SLS un-notched specimens fabricated in the Vert-x or Z-x directions, respectively. The yellow circle and purple cross are the SLS notched specimens fabricated in the Vert-x or Z-x directions, respectively. The green diamond and blue triangle are the un-notched and notched injection molded specimens. Solid color points and circled points represent run-out data (For interpretation of the references to colour in this figure legend, the reader is referred to the web version of this article).

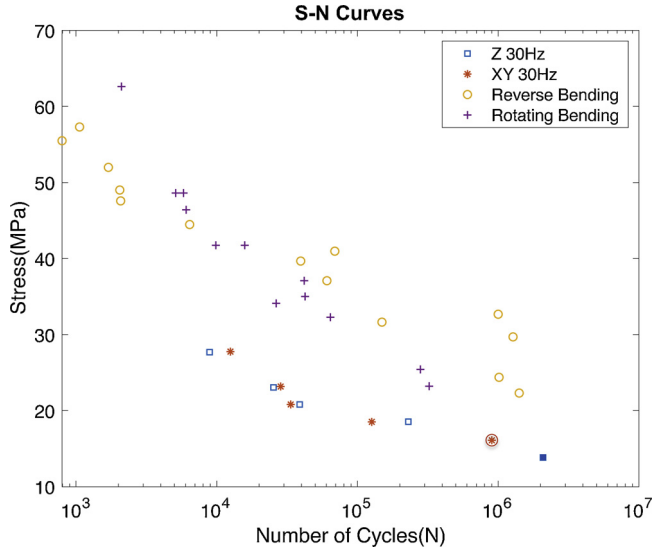

Fig. 12. The S-N curves of the best results from [71] and [72] that each printed specimen made out of PA12. The blue square and red star are the curves for hourglass specimens that were printed along the z-axis and x-axis, respectively, and were tested at a frequency of 30 Hz. The yellow circle and purple cross curves represent specimens tested with reverse bending fatigue and rotating bending fatigue. Solid color points and circled points represent run-out data (For interpretation of the references to colour in this figure legend, the reader is referred to the web version of this article).

rectilinear boxes ($35 \times 5 \times 1.4$ mm^3) of polycaprolactone (PCL). The study found that a combination of smaller particles and large laser energy densities leads to a higher degree of sintering and improved fatigue life (Fig. 13). The curve with the combination of small particles and a large energy density started off at a higher stress variation value, meaning that the specimen initially started off more rigid than the other specimens (Fig. 13). This implies that a higher degree of sintering

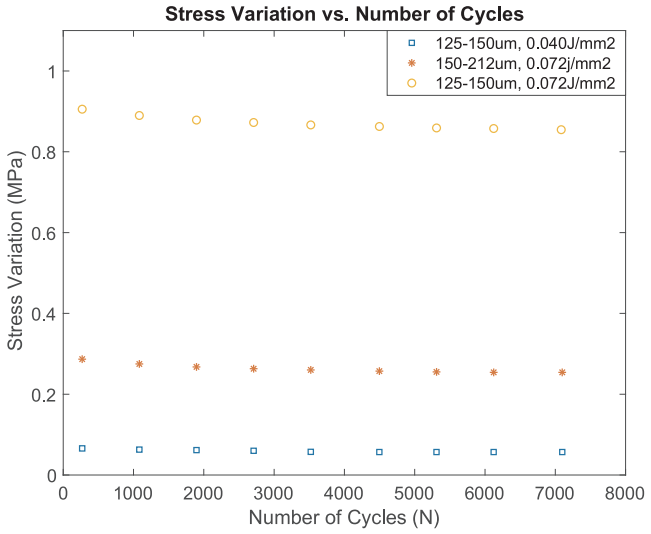

Fig. 13. The results from [75] showing the stress variation vs. number of cycles for three different combinations of particle size and laser energy density. The smaller particles were between 125 and 150 μm, and the larger particles were between 150 and 212 μm. The smaller laser energy density was 0.040 J/mm^2, while the larger energy density was 0.072 J/mm^2. The blue squares had a combination of small particles and a large laser energy density, the red star curve had smaller particles and a smaller laser energy density, while the yellow circles had a combination of large particles with a large laser energy density (For interpretation of the references to colour in this figure legend, the reader is referred to the web version of this article).

melted the particles together better, and, as a result, the fatigue life of the specimens was improved.

The studies reported in [74] and [75], investigated how affinity between two particle types affected fatigue life. In the first study [74], rectilinear boxes (35×5x1.4 mm^3) were fabricated with a mixture of Polyamide 6 (PA6) and PA12. It was found that the 20/80 and 50/50 blends had the best fatigue life, but overall there was poor affinity between the two particles (Fig. 14). Since the stress variation between the two particles was negative, it meant that the stiffness of the

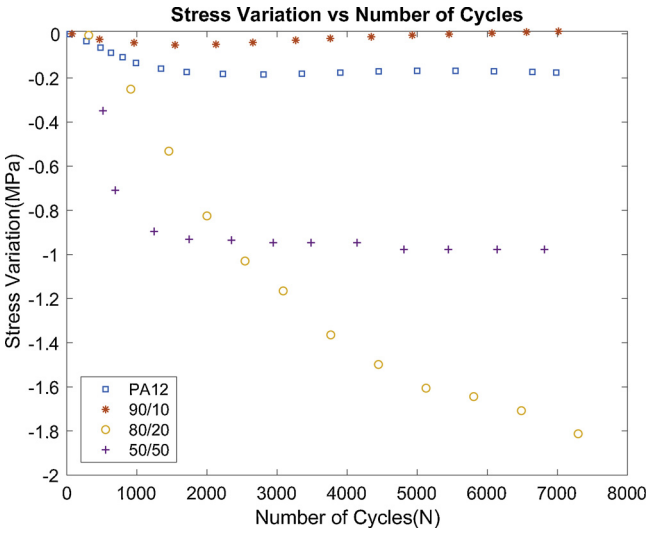

Fig. 14. The results of the best combinations of powders from [76] and [77], showing stress variation vs. number of cycles. As a control, the curve with only PA12 is represented by blue squares. The combination of PA12/PBT at 90/10 is shown with the red stars. The yellow circle and purple cross curves are PA6/PA12 blends of 80/20 and 50/50, respectively (For interpretation of the references to colour in this figure legend, the reader is referred to the web version of this article).

specimen was decreasing, leading to a poor fatigue life (Fig. 14). Similarly, [75] fabricated rectilinear boxes of PA12 and BASF polybutylene terephthalate (PBT). The blend of 90/10 had the best fatigue life (Fig. 14). The stress variation in the 90/10 blend stayed relatively constant, meaning that the specimen was neither hardening or softening under cyclic loading.

6.2.4. Fracture mechanical fatigue

Several studies investigated how different material properties affected fracture fatigue life by comparing 3D printed and injection-molded specimens, varying materials, and changing environments. In [76], compact tension specimens [77] made of PA12 were built with 3D printing and injection molding. The results found that the SLS parts had longer fatigue lives, with less deformation. In [78], compact tension specimens ($50 \times 48 \times 10$ mm^3), made of neat PA12 (PA12) and short glass fiber PA12 (PA12-f), were tested in a dry environment at 23 °C and -50 °C. At 23 °C, both materials had similar fatigue lives, but PA12-f had greatly improved fatigue life at -50 °C. In [79], compact tension specimens ($50 \times 48 \times 10$ mm^3) were fabricated of PA12 and PA11, a bio-based polymer, and tested in a dry environment at 23 °C, a dry environment at 50 °C, and a wet environment at 23 °C. Independent of the temperature and environment, PA11 showed improved fatigue crack propagation. Testing in water significantly reduced the fatigue life for both samples.

6.3. Material jetting

6.3.1. Axial loading fatigue

In one study, [80], the effects of build orientation were investigated in parts printed with a material jetting printer. Veroclear 720 dog bone specimens [41] were fabricated parallel to the X and Y-axes (Fig. 5), and cycled at 20 Hz. Veroclear 720 is a translucent, rigid acrylic-based photopolymer produced by Stratasys. The specimens that were fabricated parallel to the Y-axis (Fig. 5) had better fatigue resistance, but more experimentation was required to have statistical validity.

Material properties, such as material interfaces and surface treatments, were investigated to see how they affect the fatigue life. In two studies reported in [81] and [82], dog bone specimens [83] were fabricated using TangoBlackPlus and VeroWhitePlus. The first study [81], examined the effects of no interface, a single interface, and a dual interface on the fatigue life. TangoBlackPlus is an elastomeric acrylic-based photopolymer fabricated by Stratasys. The results of the study indicated that interface specimens do not have a shorter fatigue life as compared with the pure material itself. In a continuation study [82], dual interface specimens were used to see how surface finish affects the fatigue life. It was found that smoother, “glossy” finish specimens had a longer fatigue life as compared to matte finish, though not statistically significant.

7. Discussion

7.1. Extrusion-based printing

Throughout the literature for fatigue of extrusion-based printing, it appeared that printing and material parameters all affect the fatigue life of specimens. Focusing on printing parameters, it was found that the raster orientation had the most influence on the fatigue life. All of the studies investigating raster orientation concurred that printing at 0° (Fig. 4A) or 90° (Fig. 4B) resulted in the worst fatigue life than printing at 45° (Fig. 4C) or 45/45° (Fig. 4D). One possibility as to why 45/45° had the best fatigue life is that in uniaxial loading shear tends to occur at an angle of 45°, but during loading it is constantly counteracted by the -45° configuration [47]. This development could delay or prevent a crack from fully propagating through the material. Another possibility is that as the specimens are cyclically loaded, the 45/45° configuration start to rotate into a 0/90° orientation, resulting in the structure being better aligned with the loading direction so strand strength becomes more prevalent [47]. Aside from raster orientation, other parameters such as the printing orientation, layer height, and infill all influence the fatigue life. Printing orientation determines the stress-carrying direction, layer height affects the cohesion between the layers, and infill affects the stiffness and density of the part, all of which impact how the material behaves during fatigue testing [60]. Due to the synergy between all of the parameters, it was challenging to characterize the best settings for maximizing the fatigue life. While the general consensus between studies was that printing with 45/45° (Fig. 4D) results in the best fatigue life, the best settings for the remainder of the printing parameters remain inconclusive.

The material parameters did not seem to have as substantial of an influence as the printing parameters due to the inconclusive nature of the results. Examining whether or not injection molding or 3D printed parts had better fatigue life yielded two conflicting results. This may be due to the differing printing parameters chosen by each study, where changing printing parameters could generate a different outcome. Looking at the chosen materials throughout the literature seemed to be inconclusive as to whether ABS or PLA had the best fatigue resistance. This can be seen in Figs. 6,7, and 9, in which ABS specimens typically had the longest fatigue life, but there were also instances where PLA has the best fatigue resistance. This fluctuation in which material is better may be due to the different printing parameters each test has used, which affect the mechanical behavior of the specimen.

7.2. Selective laser sintering

As with extrusion-based printing, both printing parameters and material properties impacted the fatigue life of SLS parts. Looking at the printing parameters, several studies concluded that the printing orientation did not affect the fatigue life, since there was as an isotropic material response. This can been seen in Figs. 11 and 12. This isotropic response may be due to the localized heating and deformation that cause a uniform microstructure at the eventual fracture site through in situ drawing and/or an annealing process [70]. Another printing parameter that affects fatigue is the laser energy density, which was tested in [73]. Laser energy density affects the mechanical properties, such as porosity and microstructure, of parts built using SLS. As the laser energy density is increased, the degree of sintering increases, which leads to a denser morphology in parts.

Unlike extrusion-based printing, the material properties seemed to have a larger impact on fatigue life of SLS polymers. Throughout the literature, there seemed to be a consensus in SLS parts that an increase in the density leads to better fatigue resistance. This can be seen in Figs. 10 and 13. The density of the SLS parts influences the mechanical properties, and at lower densities, with more unfused powder particles, there is a higher chance of crack initiation [66]. Looking at the differences in the injection molded and 3D printed parts did not lead to a definitive conclusion of one method being better than the other, as seen in Fig. 11. The fatigue lives of both parts were found to be similar, with neither one having significantly better fatigue resistance. The affinity of two powders was essential to the success of the part. As can be seen in Fig. 14, when there is poor affinity between powders, the part begins to lose stiffness and fail sooner. Finally, the majority of the studies used PA12 due to its desirable mechanical properties. It is interesting to note that the PA12/PBT blend of 90/10 had a higher fatigue strength than pure PA12 due to the addition of 10% PBT, which leads to an increase in stiffness and resistance to plastic deformation.

7.3. Material jetting

Due to the limited number of studies on material jetting, only material properties were investigated. As previously mentioned, the studies found that interface specimens did not have shorter fatigue lives as compared with no interface specimens, and that although the ‘glossy’

surface had better fatigue resistance, it was not statistically relevant. This might be due to the lower roughness of the glossy surface as compared to the matt surface [84]. A lower roughness decreases the potential sites of crack initiation [86].

7.4. General remarks

As is clear from the previous chapters, there is no clear answer as to which 3D printing technique or set of printing parameters results in parts that are optimized for maximum fatigue performance. Many of the relevant parameters strongly depend on the 3D printing process and the polymer used. For every polymer, a set of specimens fabricated with different processing parameters should be tested for fatigue following experimental design techniques such as Taguchi that allow for fractional factorial designs [84]. Other optimization processes include the full factorial, gray relational, artificial neural network (ANN), fuzzy logic, genetic algorithm (GA), and response surface methodology (RSM) and have been used for different outputs like part strength, surface quality, dimension accuracy, etc. [85]. Most of these techniques have not been used for fatigue analyses but could also be considered. The slicing algorithm used is another parameter that has not been investigated thoroughly and could have a significant effect on the mechanical properties of the resulting parts.

8. Conclusions

In this literature review, the aim was to interpret all of the papers to see, whether there are trends in the data that could lead to conclusions about which printing parameters and material properties resulted in the best fatigue life. For extrusion-based printing, it was found that printing with a 45/45° raster orientation had the best fatigue life, while it was inconclusive as to if ABS or PLA was the most fatigue resistant material. The synergy between all of the printing parameters such as printing orientation, raster orientation, layer height, and infill made it challenging to determine the best parameters. In selective laser sintering, the printing orientation did not have an impact on the fatigue life of the specimens, with the specimens showing isotropic behavior. Higher densities in the parts also led to better fatigue resistance. In both extrusion-based printing and selective laser sintering, there was not enough information to determine if 3D printing yielded better fatigue results as compared with injection molding. Due to the lack of testing of parts made by material jetting, no conclusions could be made. While some conclusions about the influence of the printing parameters and material properties were made, there still is a need for more fatigue testing of 3D printed polymers. Understanding the mechanical properties of 3D printed polymers could aid in predicting and preventing fatigue failure.

References

[1] J.R.C. Dizon, A.H. Espera, Q.Y. Chen, R.C. Advincula, Mechanical characterization of 3D-printed polymers, Addit. Manuf. 20 (2018) 44–67.
[2] E. Macdonald, R. Salas, D. Espalin, M. Perez, E. Aguilera, D. Muse, R.B. Wicker, 3D printing for the rapid prototyping of structural electronics, IEEE Access 2 (2014) 234–242.
[3] S.E. Bakarich, R. Gorkin, M.I.H. Panhuis, G.M. Spinks, Three-dimensional printing Fiber reinforced hydrogel composites, Acs. Appl. Mater. Interfaces 6 (18) (2014) 15998–16006.
[4] J.L. Ifkovits, J.A. Burdick, Review: photopolymerizable and degradable biomaterials for tissue engineering applications, Tissue Eng. 13 (10) (2007) 2369–2385.
[5] S.J. Kalita, S. Bose, H.L. Hosick, A. Bandyopadhyay, Development of controlled porosity polymer-ceramic composite scaffolds via fused deposition modeling, Mater. Sci. Eng. C-Bio. Sci. 23 (5) (2003) 611–620.
[6] F.P.W. Melchels, J. Feijen, D.W. Grijpma, A review on stereolithography and its applications in biomedical engineering, Biomaterials 31 (24) (2010) 6121–6130.
[7] V.B. Morris, S. Nimbalkar, M. Younesi, P. McClellan, O. Akkus, Mechanical properties, Cytocompatibility and manufacturability of chitosan:PEGDA hybrid-gel scaffolds by stereolithography, Ann. Biomed. Eng. 45 (1) (2017) 286–296.
[8] S.V. Murphy, A. Atala, 3D bioprinting of tissues and organs, Nat. Biotechnol. 32 (8) (2014) 773–785.
[9] F. Rengier, A. Mehndiratta, H. von Tengg-Kobligk, C.M. Zechmann, R. Unterhinninghofen, H.U. Kauczor, F.L. Giesel, 3D printing based on imaging data: review of medical applications, Int. J. Comput. Assist. Radiol. Surg. 5 (4) (2010) 335–341.
[10] G.H. Wu, S.H. Hsu, Review: polymeric-based 3D printing for tissue engineering (vol 35, pg 285, 2015), J. Med. Biol. Eng. 36 (2) (2016) 284-284.
[11] R. Liu, Z. Wang, T. Sparks, F. Liou, J. Newkirk, Aerospace applications of laser additive manufacturing, Woodh. Pub. Ser. Elect. (88) (2017) 351–371.
[12] R. Melnikova, A. Ehrmann, K. Finsterbusch, 3D printing of textile-based structures by fused Deposition Modelling (FDM) with different polymer materials, Iop. Conf. Ser.-Mater. Sci. 62 (2014).
[13] R.H. Sanatgar, C. Campagne, V. Nierstrasz, Investigation of the adhesion properties of direct 3D printing of polymers and nanocomposites on textiles: effect of FDM printing process parameters, Appl. Surf. Sci. 403 (2017) 551–563.
[14] J.W. Stansbury, M.J. Idacavage, 3D printing with polymers: challenges among expanding options and opportunities, Dent. Mater. 32 (1) (2016) 54–64.
[15] J.Y. Lee, J. An, C.K. Chua, Fundamentals and applications of 3D printing for novel materials, Appl. Mater. Today 7 (2017) 120–133.
[16] J.V. Crivello, E. Reichmanis, Photopolymer materials and processes for advanced technologies, Chem. Mater. 26 (1) (2014) 533–548.
[17] J.S. Mohammed, Applications of 3D printing technologies in oceanography, Methods Oceanogr. 17 (2016) 97–117.
[18] W. Gao, Y.B. Zhang, D. Ramanujan, K. Ramani, Y. Chen, C.B. Williams, C.C.L. Wang, Y.C. Shin, S. Zhang, P.D. Zavattieri, The status, challenges, and future of additive manufacturing in engineering, J. Technol. Comput. Aided Des. Tcad 69 (2015) 65–89.
[19] A.M. Forster, Materials Testing Standards for Additive Manufacturing of Polymer Materials: State of the Art and Standards Applicability, US Department of Commerce, National Institute of Standards and Technology, 2015.
[20] L. Pruitt, L. Bailey, Factors affecting near-threshold fatigue crack propagation behavior of orthopedic grade ultra high molecular weight polyethylene, Polymer 39 (8-9) (1998) 1545–1553.
[21] J.A. Sauer, M. Hara, Effect of molecular variables on crazing and fatigue of polymers, Crazing Polym. 2 (1990) 69–118.
[22] R.J. Crawford, P.P. Benham, Some fatigue characteristics of thermoplastics, Polymer 16 (12) (1975) 908–914.
[23] R.W. Hertzberg, R.P. Vinci, J.L. Hertzberg, Deformation and Fracture Mechanics of Engineering Materials, Wiley, 2012.
[24] I. Constable, J.G. Williams, D.J. Burns, Fatigue and cyclic thermal softening of thermoplastics, Arch. J. Mech. Eng. Sci. 12 (1) (1970) 20–29.
[25] R.J. Crawford, P.P. Benham, Cyclic stress fatigue and thermal softening failure of a thermoplastic, J. Mater. Sci. 9 (1) (1974) 18–28.
[26] J.A. Sauer, G.C. Richardson, Fatigue of polymers, Int. J. Fract. Mech. 16 (6) (1980) 499–532.
[27] M.T. Takemori, Polymer fatigue, Annu. Rev. Mater. Sci. 14 (1984) 171–204.
[28] J. Schijve, Fatigue of structures and materials in the 20th century and the state of the art, Int. J. Fatigue 25 (8) (2003) 679–702.
[29] P. Chowdhury, H. Sehitoglu, Mechanisms of fatigue crack growth - a critical digest of theoretical developments, Fatigue Fract. Eng. Mater. Struct. 39 (6) (2016) 652–674.
[30] J.M. Schultz, Fatigue behavior of engineering polymers, Treat. Mater. Sci. Technol. 10 (1977) 599–636.
[31] W. Weibull, Fatigue Testing and Analysis of Results Elsevier, (2013).
[32] A.Sf. Metals, Atlas of Fatigue Curves, ASM International, 1985.
[33] K.R. Chandran, Mechanical fatigue of polymers: a new approach to characterize the SN behavior on the basis of macroscopic crack growth mechanism, Polymer 91 (2016) 222–238.
[34] K.C. Ang, K.F. Leong, C.K. Chua, M. Chandrasekaran, Investigation of the mechanical properties and porosity relationships in fused deposition modelling-fabricated porous structures, Rapid Prototyp. J. 12 (2) (2006) 100–105.
[35] A. Equbal, A.K. Sood, S.S. Mahapatra, Prediction of dimensional accuracy in fused deposition modelling: a fuzzy logic approach, Int. J. Product. Qual. Manag. 7 (1) (2010) 22–43.
[36] A.K. Sood, R.K. Ohdar, S.S. Mahapatra, Parametric appraisal of mechanical property of fused deposition modelling processed parts, Mater. Des. 31 (1) (2010) 287–295.
[37] A.K. Sood, R.K. Ohdar, S.S. Mahapatra, Experimental investigation and empirical modelling of FDM process for compressive strength improvement, J. Adv. Res. 3 (1) (2012) 81–90.
[38] H. Zarringhalam, N. Hopkinson, N.F. Kamperman, J.J. de Vlieger, Effects of processing on microstructure and properties of SLS Nylon 12, Mater. Sci. Eng. a-Struct. 435 (2006) 172–180.
[39] ASTM, D7774-17 Standard Test Method for Flexural Fatigue Properties of Plastics, ASTM International West Conshohocken, PA, (2017).
[40] ASTM, D3479/D3479M-12 Standard Test Method for Tension-Tension Fatigue of Polymer Matrix Composite Materials, ASTM International West Conshohocken, PA, (2012).
[41] ASTM, D7791-12 Standard Test Method for Uniaxial Fatigue Properties of Plastics, ASTM International, West Conshohocken, PA, (2017).
[42] ISO, 13003:2003 Fibre-reinforced Plastics – Determination of Fatigue Properties Under Cyclic Loading Conditions, ISO, Switzerland, (2003).
[43] ASTM D6115-97(2011) Standard Test Method for Mode I Fatigue Delamination Growth Onset of Unidirectional Fiber-Reinforced Polymer Matrix Composites, ASTM International West Conshohocken, PA, 2011.
[44] ISO, 15850:2014 Plastics – Determination of tension-tension Fatigue Crack Propagation – Linear Elastic Fracture Mechanics (LEFM) Approach, ISO, Switzerland, (2014).

[45] ASTM, E739-10 Standard Practice for Statistical Analysis of Linear or Linearized Stress-Life (S-N) and Strain-Life (ε-N) Fatigue Data, ASTM International, West Conshohocken, PA, 2015.
[46] C.W. Ziemian, M. Sharma, S. Ziemian, Anisotropic mechanical properties of ABS parts fabricated by fused deposition modelling, Mech. Eng., InTech (2012).
[47] S. Ziemian, M. Okwara, C.W. Ziemian, Tensile and fatigue behavior of layered acrylonitrile butadiene styrene, Rapid Prototyp. J. 21 (3) (2015) 270–278.
[48] C.W. Ziemian, R.D. Ziemian, K.V. Haile, Characterization of stiffness degradation caused by fatigue damage of additive manufactured parts, Mater. Des. 109 (2016) 209–218.
[49] ASTM D638-10 Standard Test Method for Tensile Properties of Plastics, ASTM International West Conshohocken, PA, 2010.
[50] T. Letcher, M. Waytashek, Material property testing of 3d-Printed specimen in Pla on an entry-level 3d printer, Proc. Asme Int. Mech. Eng. Cong. Expos. Vol 2a (2014) (2014).
[51] M.F. Afrose, S.H. Masood, P. Lovenitti, M. Nikzad, I. Sbarski, Effects of part build orientations on fatigue behaviour of FDM-Processed PLA material, Prog. Addit. Manuf. 1 (1-2) (2016) 21–28.
[52] J. Lee, A. Huang, Fatigue analysis of FDM materials, Rapid Prototyp. J. 19 (4) (2013) 291–299.
[53] UNI EN ISO, 527-1 Plastics-Determination of Tensile Properties-General Principles, Italy, (1977).
[54] T. Corbett, T. Kok, C. Lee, J. Tarbutton, Identification of Mechanical and Fatigue Characteristics of Polymers Fabricated by Additve Manufacturing Process, Proc. 2014 ASPE Spring Topical Meeting: Dimensional Accuracy and Surface Finish in Additive Manufacturing. (2014).
[55] M.M. Padzi, M.M. Bazin, W.M.W. Muhamad, Fatigue characteristics of 3D printed acrylonitrile butadiene styrene (ABS), 4th International Conference on Advanced Materials, Mechanics and Structural Engineering (4th Ammse 2017) 269 (2017) (2017).
[56] A.T. Miller, D.L. Safranski, K.E. Smith, D.G. Sycks, R.E. Guldberg, K. Gall, Fatigue of injection molded and 3D printed polycarbonate urethane in solution, Polymer 108 (2017) 121–134.
[57] M. Fischer, V. Schoppner, Fatigue behavior of FDM parts manufactured with ultem 9085, JomUs 69 (3) (2017) 563–568.
[58] A.T. Miller, D.L. Safranski, C. Wood, R.E. Guldberg, K. Gall, Deformation and fatigue of tough 3D printed elastomer scaffolds processed by fused deposition modeling and continuous liquid interface production, J. Mech. Behav. Biomed. Mater. 75 (2017) 1–13.
[59] B.M. Gong, S.H. Cui, Y. Zhao, Y.T. Sun, Q. Ding, Strain-controlled fatigue behaviors of porous PLA-based scaffolds by 3D-printing technology, J. Biomater. Sci.-Polym. E 28 (18) (2017) 2196–2204.
[60] G. Gomez-Gras, R. Jerez-Mesa, J.A. Travieso-Rodriguez, J. Lluma-Fuentes, Fatigue performance of fused filament fabrication PLA specimens, Mater. Des. 140 (2018) 278–285.
[61] H.Y. Zhang, L.L. Cai, M. Golub, Y. Zhang, X.H. Yang, K. Schlarman, J. Zhang, Tensile, creep, and fatigue behaviors of 3D-printed acrylonitrile butadiene styrene, J. Mater. Eng. Perform. 27 (1) (2018) 57–62.
[62] F. Arbeiter, M. Spoerk, J. Wiener, A. Gosch, G. Pinter, Fracture mechanical characterization and lifetime estimation of near-homogeneous components produced by fused filament fabrication, Polym. Test. 66 (2018) 105–113.
[63] B. Van Hooreweder, J.P. Kruth, High cycle fatigue properties of selective laser sintered parts in polyamide 12, Cirp. Annu.-Manuf. Technol. 63 (1) (2014) 241–244.
[64] ISO 1352 Metallic Materials - Torque-controlled Fatigue Testing, ISO, Switzerland, (2011).
[65] H. Amel, H. Moztarzadeh, J. Rongong, N. Hopkinson, Investigating the behavior of laser-sintered Nylon 12 parts subject to dynamic loading, J. Mater. Res. 29 (17) (2014) 1852–1858.
[66] B. Van Hooreweder, F. De Coninck, D. Moens, R. Boonen, P. Sas, Microstructural characterization of SLS-PA12 specimens under dynamic tension/compression excitation, Polym. Test. 29 (3) (2010) 319–326.
[67] B. Van Hooreweder, D. Moens, R. Boonen, J.P. Kruth, P. Sas, On the difference in material structure and fatigue properties of nylon specimens produced by injection molding and selective laser sintering, Polym. Test. 32 (5) (2013) 972–981.
[68] H. Amel, J. Rongong, H. Mortarzadeh, N. Hopkinson, Effect of section thickness on fatigue performance of laser sintered nylon 12, Polym. Test. 53 (2016) 204–210.
[69] J. Munguia, K. Dalgarno, Fatigue behaviour of laser-sintered PA12 specimens under four-point rotating bending, Rapid Prototyp. J. 20 (4) (2014) 291–300.
[70] J. Munguia, K. Dalgarno, Fatigue behaviour of laser sintered Nylon 12 in rotating and reversed bending tests, Mater. Sci. Technol.-Lond. 31 (8) (2015) 904–911.
[71] BS 3518-3 Methods of Fatigue Testing: Direct Stress Fatigue Tests, British Standards Institution, (1963).
[72] ASTM D671-93 Standard Test Method for Flexural Fatigue of Plastics by Constant-Amplitude-of-Force (Withdrawn 2002), ASTM International West Conshohocken, PA, 1993.
[73] G.V. Salmoria, D. Hotza, P. Klauss, L.A. Kanis, C.R.M. Roesler, Manufacturing of porous polycaprolactone prepared with different particle sizes and infrared laser sintering conditions: microstructure and mechanical properties, Adv. Mech. Eng. (2014).
[74] G.V. Salmoria, J.L. Leite, L.F. Vieira, A.T.N. Pires, C.R.M. Roesler, Mechanical properties of PA6/PA12 blend specimens prepared by selective laser sintering, Polym. Test. 31 (3) (2012) 411–416.
[75] G.V. Salmoria, V.R. Lauth, M.R. Cardenuto, R.F. Magnago, Characterization of PA12/PBT specimens prepared by selective laser sintering, Opt. Laser Technol. 98 (2018) 92–96.
[76] M. Blattmeier, G. Witt, J. Wortberg, J. Eggert, J. Toepker, Influence of surface characteristics on fatigue behaviour of laser sintered plastics, Rapid Prototyp. J. 18 (2) (2012) 161–171.
[77] ASTM E399-17 Standard Test Method for Linear-Elastic Plane-Strain Fracture Toughness KIc of Metallic Materials, ASTM International West Conshohocken, PA, 2017.
[78] A. Salazar, A. Rico, J. Rodriguez, J.S. Escudero, R. Seltzer, F.M.D. Cutillas, Fatigue crack growth of SLS polyamide 12: effect of reinforcement and temperature, Compos Part B-Eng. 59 (2014) 285–292.
[79] A. Salazar, A. Rico, J. Rodriguez, J.S. Escudero, R. Seltzer, F.M.D. Cutillas, Monotonic loading and fatigue response of a bio-based polyamide PA11 and a petrol-based polyamide PA12 manufactured by selective laser sintering, Eur. Polym. J. 59 (2014) 36–45.
[80] J.A. Suresh, G.S. Kumar, P. Ramu, J. Rengaswamy, Fatigue life characterization of additively manufactured acrylic like poly-jet printed parts, Adv. Struct. Integr. (2018) 623–632.
[81] J.P. Moore, C.B. Williams, Fatigue Characterization of 3D Printed Elastomer Material, 19th Annual International Solid Freeform Fabrication Symposium (SFF), (2008).
[82] J.P. Moore, C.B. Williams, Fatigue properties of parts printed by PolyJet material jetting, Rapid Prototyp. J. 21 (6) (2015) 675–685.
[83] ASTM D4482-11(2017) Standard Test Method for Rubber Property—Extension Cycling Fatigue, ASTM International West Conshohocken, PA, 2017.
[84] G. Taguchi, S. Chowdhury, Y. Wu, Taguchi's Quality Engineering Handbook, John Wiley & Sons, Hoboken, NJ, 2005.
[85] O.A. Mohamed, S.H. Masood, J.L. Bhowmik, Optimization of fused deposition modeling process parameters: a review of current research and future prospects, Adv. Manuf. 3 (1) (2015) 42–53.